Model-Based Detection and Correction of Corrupted Wavelet Coefficients

Norbert Strobel, Sanjit K. Mitra, and B.S. Manjunath *
Signal and Image Processing Laboratory
Department of Electrical and Computer Engineering
University of California, Santa Barbara 93106
Telephone: (805) 893-8312

Email: strobel@iplab.ece.ucsb.edu

Abstract

Image decomposition based on the discrete wavelet transform (DWT) has been proposed for efficient storage and progressive transmission of images for visual browsing in digital image libraries. Although the compression aspects of the DWT have been carefully researched, reconstruction errors due to corrupted wavelet coefficients have received less attention. In this paper we consider the problem of bit errors affecting uniformly quantized wavelet coefficients. The proposed method, which is based on a local image model, simultaneously detects and masks corrupted wavelet coefficients.

1 Introduction

Image compression schemes often include, as a final stage of processing, a variable word length coding operation. The bit stream generated thus consists of words which can only be unambiguously decoded, if they correspond to codebook entries. In such a situation bit errors can have a potentially catastrophic effect upon the reconstructed image. Traditional forward error correcting methods offer one solution to this problem. Their application, however, can lead to a significant increase in system complexity and bit-rate. Alternatively, fixed-length codes can be used. Although their compression performance is lower, they are inherently synchronized, and, therefore, bit errors do not spread and corrupt entire image regions. Depending upon the situation, a combination of fixed-rate methods and error concealment techniques might be appropriate.

The paper is structured as follows: Section 2 describes bit error effects, and Section 3 explains the algorithm for error detection and concealment. Experimental results are provided in Section 4, and a discussion follows in Section 5.

*This work was supported in part by NSF Grant Number IRI 94-11330.

2 Error Effects

Although the wavelet transform [1] has become a popular tool for multiresolution applications, considerably less attention has been paid to the impact of corrupted wavelet coefficients on the reconstructed picture.

It is assumed that random errors are introduced in the bits that convey information about quantizer output levels, and that these are inverted in a statistically independent manner. Coding/decoding control information (subband rates, means and quantizer bin widths), however, is considered to be error protected and hence correctly available at the receiver.

Wavelet coefficients are represented in sign-magnitude format and corrupted wavelet coefficients, i.e., coefficients whose codewords have been affected by random bit-flips, lead to characteristic error patterns as shown in Fig. 1. They are, in fact, erroneous impulse responses associated with the filters of those channels where corruption occurred. Since the filters are known, detecting and correcting corrupted wavelet coefficients involves: (1) finding local outliers (candidates for corruption), (2) testing if local singularities are truly related to corrupted wavelet coefficients (note that they could also be related to details and edges), and (3) if corrupted wavelet coefficients are detected, replacing them with an approximation of their true value. This process is repeated for each reconstruction level.

Our algorithm is designed for bit error probabilities of up to five percent, preferably less. For higher error rates, different methods should be chosen as, for example, discussed by Clarke [4].

3 Error Detection and Concealment

As indicated earlier, it is assumed that wavelet coefficients are *quantized*. Quantization, however, results in setting small wavelet coefficients to zero, and hence, in discarding fine image details and structures. It, therefore, effectively smoothes image regions and offers the

0-8186-8183-7/97 $10.00 © 1997 IEEE

Figure 1: Reconstructed image from corrupted wavelet coefficients. Corrupted wavelet coefficients appear as characteristic error patterns related to the impulse responses of associated filters.

opportunity to use a model–based approach relying on continuous, smooth surfaces, also called *facets*, to detect and conceal errors [6].

Consider a closed neighborhood, $W(r,c)$, in the pixel domain with height H, width W, and a center-deleted neighborhood, $\bar{W}(r,c)$, at location (r,c) as shown in Fig. 2. Row and column indices, denoted r and c, respectively, are taken with respect to some suitably chosen coordinate system as shown in Figs. 3 and 4. $\bar{W}(r,c)$ can be expressed as the difference between two sets, namely the closed neighborhood set, $W(r,c)$, and the center region, $W_c(r,c)$:

$$\bar{W}(r,c) = W(r,c) \setminus W_c(r,c). \tag{1}$$

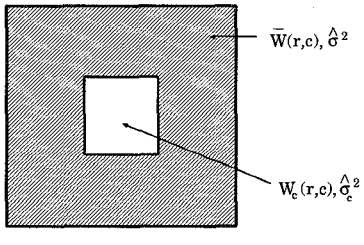

Figure 2: Center-deleted neighborhood $\bar{W}(r,c)$. The closed neighborhood $W(r,c)$ is the union of $\bar{W}(r,c)$ and $W_c(r,c)$.

The dimensions of the center window $W_c(r,c)$ have to be chosen such that it covers the entire filter support or at least the region where most of the filter energy is concentrated.

To reduce the number of false positives (type I errors) and to avoid unnecessary operations, we first test if the center region $W_c(r,c)$ is likely to originate from a corrupted wavelet coefficient, and therefore, warrants

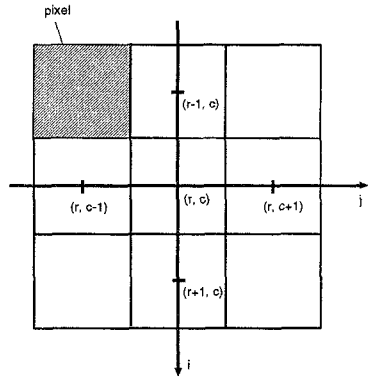

Figure 3: Coordinate system aligned with pixel center.

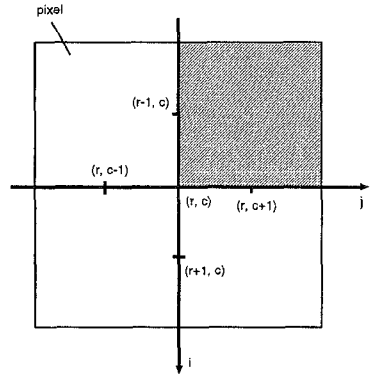

Figure 4: Coordinate system aligned with pixel boundaries.

further tests. This step involves a rank-ordering operation among the gray levels contained in $W_c(r,c)$ and $\bar{W}(r,c)$. As a result, we obtain (center) coefficients $x_{c,i}$, $i = 1 \ldots N_c$, such that $x_{c,i} \leq x_{c,i+1}$. Similarly the center deleted neighborhood yields coefficients x_i, $i = 1 \ldots N$, which satisfy $x_i \leq x_i + 1$. We consider the center region $W_c(r,c)$ corrupted, if (1): $x_{c,1} < x_1$, or (2): $x_{c,N_c} > x_N$. More sophisticated tests could involve linear combinations of the rank-ordered gray values [7].

Corrupted regions are then further investigated using the slope-facet model:

$$g(r,c) = ur + vc + w + \eta(r,c). \tag{2}$$

where $\eta(r,c)$ is assumed to be an independent additive Gaussian noise having zero mean and variance σ^2. The slope-facet model serves as a local approximation of the underlying pixel intensity $f(r,c)$. The estimated model parameters, called $\hat{u}$, $\hat{v}$, and $\hat{w}$, are then obtained using a least squares approach, i.e., via minimizing:

$$\epsilon^2 = \sum_{(i,j)\in\bar{W}(r,c)} [\hat{u}i + \hat{v}j + \hat{w} - f(r-i, c-j)]^2. \tag{3}$$

Without loss of generality assume the center of $\bar{W}(r,c)$ as the origin of the relative coordinate system for each neighborhood, i.e.,

$$\sum_{(i,j)\in\bar{W}(r,c)} i = 0, \text{ and}$$
$$\sum_{(i,j)\in\bar{W}(r,c)} j = 0.$$

Two coordinate systems are considered: Fig. 3 shows an example that is aligned with pixel centers and used to describe odd-size local neighborhoods. Fig. 4 depicts its pixel boundary aligned counterpart, suitable for indexing even-size neighborhoods.

For brevity we use the short-hand notation $\sum_{\bar{W}}$ for $\sum_{(i,j)\in\bar{W}(r,c)}$. It is implicitly understood that the corresponding row and column indices are taken from $\bar{W}(r,c)$. Then $\hat{u}$, $\hat{v}$, and $\hat{w}$ are given by:

$$\hat{u} = \frac{\sum_{\bar{W}} f(r-i,c-j)\cdot i}{\sum_{\bar{W}} i^2} \quad (4)$$

$$\hat{v} = \frac{\sum_{\bar{W}} f(r-i,c-j)\cdot j}{\sum_{\bar{W}} j^2} \quad (5)$$

$$\hat{w} = \frac{\sum_{\bar{W}} f(r-i,c-j)}{N} \quad (6)$$

As a result, the slope–facet model estimate becomes

$$\hat{g}(r,c) = \hat{u}r + \hat{v}c + \hat{w} + \eta(r,c). \quad (7)$$

To investigate whether the center region $W_c(r,c)$ should be considered as corrupted or not, we use center differences $\delta_c(.)$ taken between the pixels contained in $W_c(r,c)$ and their reference values based on the slope-facet model. More precisely, $\forall\,(i,j) \in W_c(r,c)$

$$\delta_c(r-i,c-j) := \hat{g}(r-i,c-j) - f(r-i,c-j). \quad (8)$$

If $W_c(r,c)$ does not result from a corrupted wavelet coefficient, then it can be shown that all center differences have a zero-mean Gaussian distribution and that the expected value of the sum of their squared values is lower bounded by $\sigma^2\, N_c(1+1/N)$ where N_c denotes the number of elements in $W_c(r,c)$. As a result, the sum of squared center differences can be used to obtain a center-based, conservative estimate of the noise variance called, $\hat{\sigma}_c^2$, given by:

$$\hat{\sigma}_c^2 = \frac{N/N_c}{N+1} \sum_{(i,j)\in W_c} \delta_c^2(r-i,c-j). \quad (9)$$

It can be shown that the slope facet model taken over $\bar{W}(r,c)$ offers another way to arrive at an estimate $\hat{\sigma}^2$ of the noise variance σ^2:

$$\hat{\sigma}^2 = \frac{\epsilon^2}{N-3}. \quad (10)$$

Eq. (10) can be easily verified by applying the expected value operator to Eq. (3).

Comparison of the (center difference) variance $\hat{\sigma}_c^2$ with the variance $\hat{\sigma}^2$ of the reference neighborhood $\bar{W}(r,c)$ offers a test to detect whether the center region is likely to be corrupted or not. In other words, if

$$t := \frac{\hat{\sigma}_c^2}{\hat{\sigma}^2} \quad (11)$$

exceeds a suitably chosen threshold T, the center region is considered to be the result of a corrupted wavelet coefficient and investigated further. Exploiting the fact that a corrupted wavelet coefficient will be represented by the impulse response of its associated filter, a template matching operation is used to finally decide if corruption occurred and which subband it affected. If an erroneous center region, $W_c(r,c)$, is detected, we correct all associated pixels by estimating their original values based on pixels in the neighborhood.

4 Experimental Results

We now present the results of an experiment obtained using a Haar wavelet decomposition of the camera man image. Quantization is performed by first subtracting off the mean of each subband and then by finding bits and bin widths for each uniform quantizer such that, given an average precision of, for example, 4 bits/coefficient, the overall mean square error is minimized. Note that no entropy encoding has been performed for reasons discussed earlier. The peak signal to noise ratio (PSNR) for the camera man reconstruction based on uncorrupted wavelet coefficients is 35.31 dB. The wavelet coefficients are stored in sign-magnitude format and corruption is simulated by randomly flipping bits with a given (error) probability. Fig. 5 shows a wavelet reconstruction taken over one level where 2% of the underlying coefficients are corrupted. As a result, the PSNR of the reconstructed (noisy) image fell to 23.87 dB. Due to the Haar filter pair the resulting error patterns after reconstruction are of size 2×2. Note that since the LL-band contains most of the image energy, related bit errors are more noticeable than those resulting from corrupted LH-, HL-, or HH-band coefficients.

The reconstruction result after error concealment is shown in Fig. 6 where a decision threshold $T = 4$ was used. We see that most of the corrupted areas have been masked while most of the noticeably significant image details have been kept. The PSNR after error concealment improved by approximately 6.0 dB to 29.99 dB. However, some corrupted regions have not been removed. This problem either occurs along edges or when neighboring wavelet coefficients are corrupted. In both cases the slope-facet model no longer serves as a good reference for the underlying image region.

Figure 5: Reconstructed image with 2% corrupted wavelet coefficients.

Figure 6: Camera man after error concealment.

5 Discussion and Conclusions

A model–based approach to conceal bit errors affecting wavelet coefficients has been presented. This method works satisfactorily well for very low error rates but cannot deal with high corruption rates. Two possible ways of improving the performance of the algorithm are as follows: First, a two-step implementation can be used where the LL-band is investigated separately. In other words, one can make use of the fact that this band resembles the original image and, as a result, apply a similar model-based detection/concealment technique to remove errors before combining it with corresponding detail signals. Such a step might reduce the number of corrupted LL-band coefficients and, hence, alleviate the problem of hard-to-detect errors when corrupted coefficients from different bands spatially coincide. Another possibility to reduce the number of corrupted wavelet coefficients is to apply the present algorithm more than once. While such a procedure reduces the amount of visible corruption, it also increases the degree of noticeable blurring.

References

[1] M. Vetterli and J. Kovacevic, "Wavelets and Subband Coding," Prentice Hall, Englewood Cliffs, NJ, 1995.

[2] N. Strobel, S.K. Mitra, and B.S. Manjunath, "An Approach to Efficient Storage, Retrieval, and Browsing of Large Scale Image Databases," Proc. SPIE Vol. 2606, Digital Image Storage and Archiving Systems, Philadelphia, Pennsylvania, October, 1995, pp. 324-35.

[3] N.S. Jayant and P. Noll, "Digital Coding of Waveforms," Prentice-Hall, Englewood Cliffs, NJ, 1984.

[4] R.J. Clarke, "Digital Compression of Still Images and Video," Academic-Press, New York, 1995.

[5] Yasuoka, Y. and R.M. Haralick, "Peak Noise Removal by a Facet Model," Pattern Recognition, vol. 16, 1983, pp. 23-29.

[6] R.M. Haralick and L.G. Shapiro, "Computer and Robot Vision," 1st ed., Addision-Wesley, Reading, MA, 1992.

[7] I. Pitas, and A.N. Venetsanopoulos, "Nonlinear Digital Filters - Principles and Applications," Kluwer, Boston, 1990.